ISSN: 1220-3173; E-ISSN: 2457-7618

MORPHOLOGICAL AND MORPHOMETRICAL FEATURES OF THE SCAPULA IN *CHLOROCEBUS SABAEUS* FROM SAINT KITTS AND NEVIS ISLANDS

CARACTERISTICI MORFOLOGICE ȘI MORFOMETRICE ALE SCAPULUI LA SPECIA *CHLOROCEBUS SABAEUS* DIN INSULELE SAINT KITTS AND NEVIS

C.O. MARTONOS[1)], W.B. LITTLE[1)], C. LAȚIU[2)], A.I. GUDEA[2),*)], F.G. STAN[2)], C.C. DEZDROBITU[1)]

ABSTRACT | REZUMAT

The present paper describes the morphological and morphometrical characteristics of the scapula in the Green Monkey (*Chlorocebus sabaeus*) from Saint Kitts and Nevis Islands. The purpose of our study is to provide a complete anatomical and morphometrical evaluation of the scapula that may serve for radiological or surgical diagnosis or interventions and to establish a reference set of comparative data for related species. Methods include the anatomical, classical approach, describing the characteristics of the bony eminences and depressions found while the morphometrical investigation tackles a series of standard and non-standard measurements and indices calculated based on these measurements. The results of our study are systematically presented as anatomical and then metrical conclusions, with the main conclusions pointing to characteristics similar to those of other monkey species, such as *S. leucopus* or some other non-human primates, with features that indicate a significant amount of adaptation for arboreal locomotion.

Keywords: vervet monkey, scapula, morphology, morphometry, osteometry

Lucrarea descrie morfologia și morfometria scapulei provenite de la Maimuța Verde de Saint-Kitts si Neville (*Chlorocebus sabaeus*). Acest tip de studiu își dorește să servească și ca mijloc ajutător pentru diagnosticul radiologic sau chiar cel chirugical și să stabilească un set de date morfologice de referință și pentru alte specii înrudite. Metoda de studiu a inclus investigația anatomică clasică, descriind caracteristicile elementelor și accidentelor de suprafață identificate cât și elementele de morfometrie care aplică o serie de măsurători standardizate, dar și nestandardizate. Au fost de asemenea calculate o serie de valori ale indecșilor metrici derivați din măsurătorile efectuate. Rezultatele investigației noastre sunt prezentate sistematic, ca date morfologice apoi morfometrice, concluziile indicând o serie de caracteristici similare altor specii de maimuțe, precum *S. leucopus* sau alte primate nonumane, cu unele caracteristici adaptative specifice locomoției arboricole.

Cuvinte cheie: maimuța verde, scapula, morfologie, morfometrie, osteometrie

Taxonomically, the *Chlorocebus sabaeus* monkey is an Old-World Monkey belonging to the genus *Chlorocebus.* Thanks to their vast geographic adaptability, these monkeys are found in many ecosystems inside the African continent. The presence of these monkeys in the Saint Kitts and Nevis Federation dates back to the colonial period, when they were imported as pets (13). Due to their prolific nature in captivity and ease of management, this species (like some other newly-introduced species) has become the most dominant non-human primate animal model utilised in a large array of biomedical research (3, 9, 23). In the area of descriptive anatomy, previous studies have focused on the anatomical features of this species' auditory ossicles (17, 15), the central nervous system and visual pathways, and the variability of shape, position, and number of the mental foraminae with the description of their skull morphology (19).

Previous literature has reported anatomical descriptions for the scapular bone in other primates such as the Gorilla (*Gorilla gorilla*)(11), Chimpanzee (*Pan troglodytes*), Orangutan (*Pongo abelii*), Gibbon (*Hylobates* sp.), Rhesus monkey (*Macaca mulatta*), White footed Tamarin (*Sanguinus leucopus*), Common marmoset (*Callithrix jacchus*), Paranthropus boisei, and Human species (*Homo sapiens sapiens*), with differing levels of description in morphological and morphometrical details. Another important problem addressed in terms of scapular morphology and shoulder mobility points to a much wider meaning of the role of upper limb adaptations in primates (16, 27, 26, 10, 5).

The goal of the present study is to provide a complete anatomical and morphometrical evaluation of

1) Ross University School of Veterinary Medicine, Basseterre, St. Kitts and Nevis
2) University of Agricultural Sciences and Veterinary Medicine Faculty of Veterinary Medicine, Cluj-Napoca, Romania
*) *Corresponding author: alexandru.gudea@usamvcluj.ro*

the scapula in the *Chlorocebus sabaeus* monkey from Saint Kitts and Nevis that may increase our knowledge in this species and serve as an initial base of comparison for morphological, radiologic diagnostics or surgical interventions of this bone in Green monkeys.

MATERIALS AND METHODS

The anatomical approach

The biological material for this research utilised five complete skeletons, which were part of a private collection owned by Mr. Roger Hancok and found on Saint Kitts Island. The owner specifically permitted the study of these specimens in the anatomy laboratory of Ross University School of Veterinary Medicine (RUS VM), Saint Kitts and Nevis, Basseterre complying with Institutional Animal Care and Use Committee (IACUC) approval #TSU10.27.2023 CM RUSVM. Examination of dentition revealed all specimens were adults, including three males (k930, k945, and k 920) and two females (a438 and v585).

Both scapulas from each specimen were used to document a predetermined list of anatomical features. Significant anatomic attributes of the lateral, medial, and ventral surfaces of the scapula were photographed and measured precisely for comparison with data reported previously in humans and other mammalian species. Anatomical terminology was used following the sixth edition of Nomina Anatomica Veterinaria 2017 (28). Images for this study were obtained with a DSLR Canon EOS 90D® and were later processed with the Adobe® Photoshop programme for fine contrast and background adding.

The morphometrical approach

The morphometrical investigation was carried out with digital callipers and measuring software tools provided by ImageJ® software. Specimens were oriented for photography with the precise positioning of a metric ruler in the same plane as the bone, such that digital images may be used for measurement as well as the physical specimen itself. Calibration for mea-

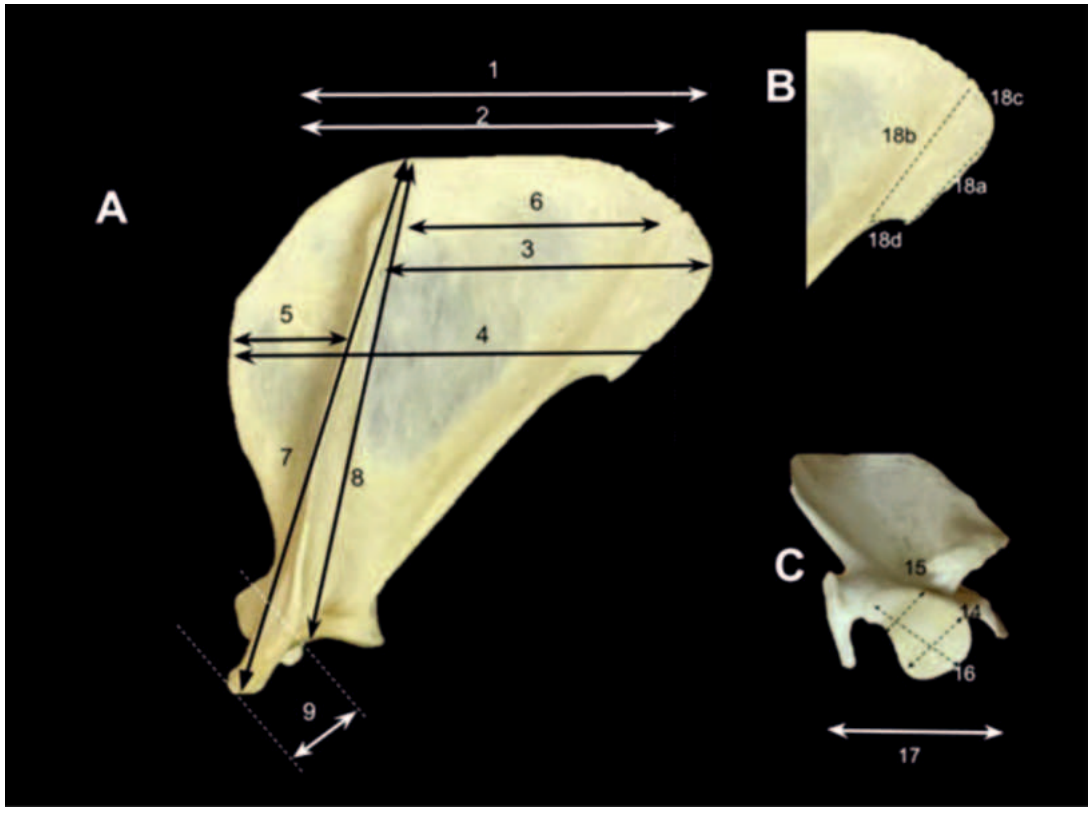

Fig. 1. Morphometric measurements of the scapula, lateral view. (A). 1) Scapular dorsal margin width without cartilage, 2) Scapular maximal width, 3) Width of infraspinous fossa, 4) Width of supraspinous fossa, 5) Total length of scapular spine, 6) Total scapular length, 7) Total length of acromion process, 8) Total length of the caudal margin. Measurements on the area of origin for m.teres major (B) 18a) caudal length, 18b) cranial length, 18c) dorsal length, 18d) ventral width Measurements on the glenoid cavity (C) 14) maximum width of the glenoid cavity, 15) minimal width of the glenoid cavity, 16) length of the glenoid cavity as the distance between the maximal cranial and caudal point of the glenoid cavity, 17) width from the coracoid process until the acromion as the distance between the acromion and the coracoid process

Table 1

List of measurements on the scapula

1 Scapular width with cartilage: distance between the cranial and cartilaginous caudal angle.
2 Scapular width without cartilage: distance between the cranial and bony caudal angle.
3 Maximal width with cartilage of scapula: distance between the maximum projection of cranial margin and cartilaginous caudal angle.
4 Maximal width without cartilage: distance between the maximum projection of the cranial margin and the bony caudal angle.
5 Width of supraspinous fossa: distance between the maximum projection of the cranial margin and spine.
6 Width of infraspinous fossa: distance between the base of the spine and the craniodorsal point of the surface for the m. teres major.
7 Projection length of scapular spine: distance between the base of the spine and the cranioventral limit of the acromion.
8 Scapular length: distance between the base of the spine and the centre of the glenoid cavity.
9a Length of acromion: distance between the craniodorsal limit of the hamatus process and the caudoventral limit of the acromion (along the long axis of the acromion).
9b Width of the acromion measured perpendicularly to the long axis under the acromi- clavicular joint.
10 Maximal length of coracoid process: distance between the base and ventral limit of the coracoid process.
11 Width of coracoid process: distance between the cranial and caudal margins of the coracoid process.
12 Cranial transverse diameter of scapular incisura: maximal distance between the ventral limit of the cranial margin and the base of the coracoid process.
13 Maximal depth of scapular incisura: distance between the cranial transverse diameter and the maximal caudal limit of the scapular incisura.
14 Maximal width of glenoid cavity: caudal diameter of cavity glenoid.
15 Minimal width of glenoid cavity: cranial diameter of cavity glenoid near supraglenoid tubercle.
16 Length of glenoid cavity: distance between the maximal cranial and caudal points of the glenoid cavity.
17 Width from coracoid process to acromion: distance between acromion and coracoid process.
18a Surface for the origin of the m. teres major: Caudal length: distance between caudodorsal and caudoventral limits of the surface for the *m. teres major*.
18b Surface for the origin of the *m. teres major*:-cranial length.
18c Surface for the origin of the *m. teres major*:-dorsal width.
18d Surface for the origin of the *m. teres major*:-ventral width.

surements was performed based on the original millimetric scale inserted into the initial photograph, and all measurements were reported in millimetres.

The following set of measurements (27, 24, 25) was attained for each bone as suggested by previous researchers (Fig. 1).

All metrical data collected (for value sets n greater than 10) were checked for normality using the Kolmogorov-Smirnov test, and basic statistical data was extracted. Differences between male and female bones were performed using the one-way Anova test (including the Tukey HSD-honesty significant difference test) (despite the reserves on such a small sample size) for independent measures, with the significance level set at less than 0.05. For measurements of area, the polygonal selection tool embedded into the same software application was utilised while following the visible anatomical landmarks.

RESULTS AND DISCUSSIONS

The scapula of the *Chlorocebus sabaeus* monkeys can be described as a flat, triangular bone (Fig. 2) that covers the cranio-lateral aspect of the rib cage. At this level, it has an oblique position with the dorsal border oriented dorso-caudally and the ventral angle oriented ventro-cranially and medio-laterally. Generally, the scapula allows for the description of its two surfaces, three borders, and three angles. The lateral surface (*Facies lateralis*) (Fig. 2), which is covered by muscles and faces mainly laterally, while the medial surface (*Facies medialis*) faces mainly medially towards the rib cage. The lateral surface had a triangular shape and with several specific anatomical entities identifiable. The most developed was the scapular spine (*Spina scapulae*), a straight bony crest that starts from the dorsal margin and descends towards the ventral angle of the scapula. It is important to note that the spine increases in height gradually from proximal to distal, where it ends with a prominent acromion (*acromion*) (Fig. 2). At the distal end of the acromion the hamatus process (*Processus hamatus*) was identified in a dorso -medial orientation. The position of this process allows it to cover the lateral surface of the glenohumeral joint

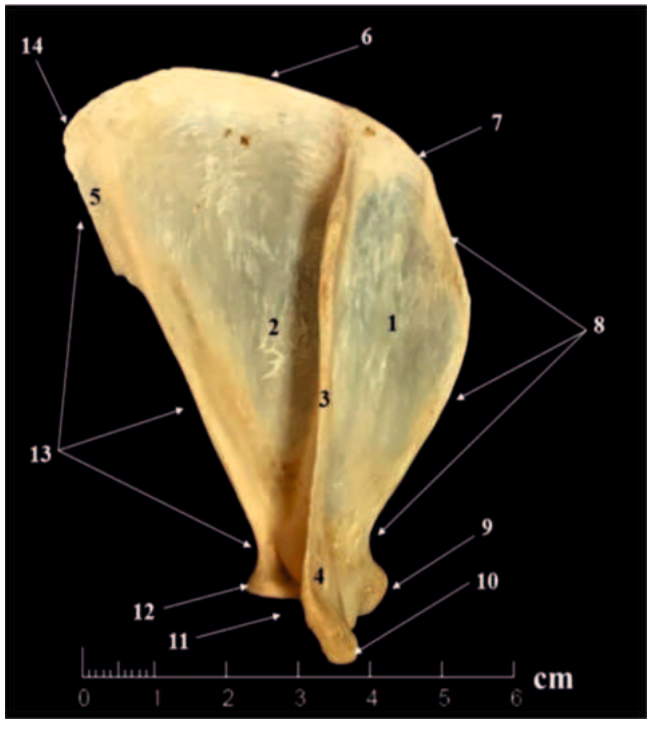

Fig. 2. Anatomical features of the lateral surface of the scapula. 1) Supraspinous fossa, 2) In-fraspinous fossa, 3) Scapular spine, 4) Acromion process, 5) Origin area for teres major muscle, 6) Dorsal border, 7) Cranial angle, 8) Cranial border, 9) Supraglenoid tubercle, 10) Hamatus process, 11) Glenoid cavity, 12) Infraglenoid tubercle, 13) Caudal border, 14) Caudal angle

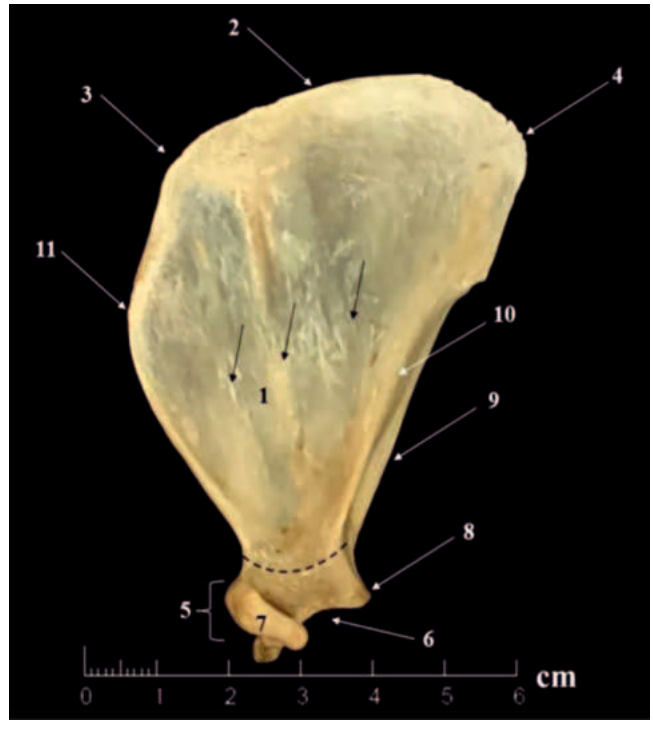

Fig. 3. Anatomical features of the medial surface of the scapula. 1)Subscapular fossa, 2) Dorsal border, 3) Cranial angle, 4) Caudal angle, 5) Ventral angle, 6) Glenoid cavity, 7) Coracoid process, 8) Infraglenoid tubercle, 9) Caudal border, 10) Supplementary line for muscular insertion, 11) Cranial border, Black arrows- bony line for muscular insertion, Dotted line- scapular neck

(*Articulatio humeri*) and articulate with the well- developed clavicular bone (*clavicula*).At this level,the acromioclavicular joint area may be identified. Dorsally and ventrally to the scapular spine, two large areas for muscular insertion were identified, the supraspinous fossa (*Fossa supraspinata*) and a larger infraspinous (*Fossa infraspinata*) fossa. The relative ratio between these two fossae was approximately 1:2 (Table 2 and 5) with the infraspinous fossa being larger (Table 2). The dorso-caudal area of the infraspinous fossa provides the point of origin for the teres major muscles (*m. teres major*). The vascular foramen in the studied specimens were located at the level of the infraspinous fossa, near the distal extremity of the bone.

The medial surface (Fig. 3) (*Facies costalis*) of the scapula had a triangular aspect and was slightly concave in nature creating the subscapular fossa (*Fossa subscapularis*). Several muscular lines could be noted, associated with the location of origin for the subscapularis muscle (*M. subscapularis*).

The cranial margin (*Mago cranialis*) of the bone had sinuous, curved appearance as the proximal third was convex cranially and the distal third was concave further distally toward the scapular notch (*Incisura scapulae*) and scapular neck (*Collum scapulae*).

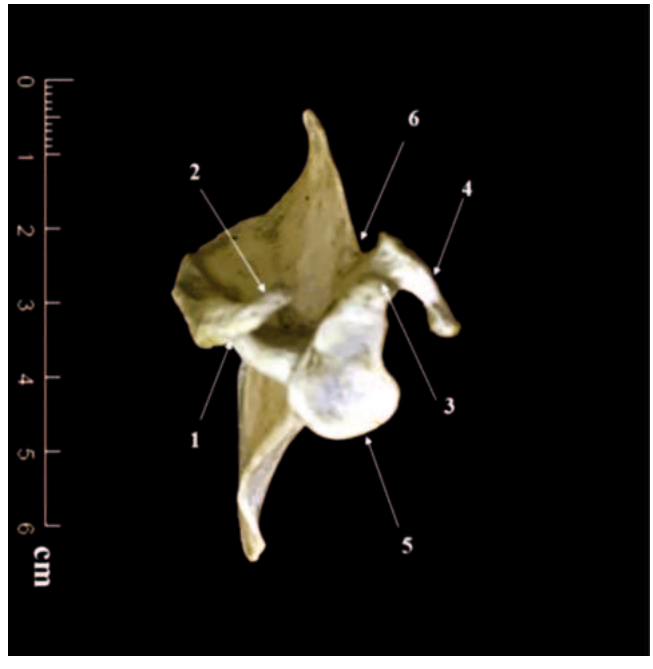

Fig. 4. Anatomical features of the ventral angle of the scapula. 1) Acromional process, 2) Hamate process, 3) Supraglenoid tubercle, 4) Coracoid process, 5) Glenoid cavity, 6) Scapular notch

Table 2

Morphometrical data for all measured specimens (length in mm)

Measurement no	Avg	St. dev	min	max	n
2	53.59	2.24	51.18	58.19	9
4	59.49	2.56	56.00	64.26	9
5	18.77	2.30	15.20	21.64	9
6	35.11	1.90	32.24	38.57	9
7	72.92	4.61	65.05	81.22	10
8	62.80	4.44	55.30	70.52	10
9 a	12.26	1.81	8.76	15.00	10
9 b	4.55	0.393	4.12	5.37	8
10	12.55	1.19	10.80	14.29	10
11	4.19	0.47	3.32	5.16	10
12	23.31	4.55	18.37	32.00	8
13	4.97	0.68	3.96	6.00	8
14	10.74	1.95	7.15	14.00	15
15	7.84	2.87	5.06	13.80	15
16	16.43	2.77	13.85	24.54	14
17	29.31	3.05	23.50	34.20	19
18 a	17.43	1.88	15.61	19.37	4
18 b	23.63	2.84	19.40	25.51	5
18 c	6.57	1.51	5.08	8.60	5
18 d	6.28	1.32	4.34	7.33	5

In a dorso-ventral direction this margin had a constant thickness throughout, serving as a muscular insertion area (Table 2). The dorsal margin (*Margo dorsalis*) had an arch appearance and curved dorsally as it attached to the scapular cartilage (*Cartilago scapulae*).

Finally, the caudal margin (*Margo caudalis*) had a straight margin with a bony projection approximately one third total length from the dorsal border. This was identified as the origin of the teres major muscle. Distal to this, a double line appearance was noted. The lateral of these two lines is the ventral continuation of the caudal part of the scapular cartilage and the medial line demarcates the caudal angle of the scapula. At this location several origins of muscles which act to flex the shoulder originate. The lateral line serves as the origin of the teres major and teres minor muscles while the medial line is the origin point for the subscapularis muscle. Marked by the above-mentioned margins, three angles of the bone are defined. The cranial angle (*Angulus cranialis*) was located between the cranial and dorsal mar-gins and displayed a convex (rounded) appearance which seems to be an adaptation to arboreal locomotion, because it increases the mobility of the entire bone [31]. The caudal angle (*Angulus caudalis*) topographically is located between the dorsal and caudal margins. Compared with the cranial angle, the caudal one has a more acute angle and serves as the origin point for the teres major muscle. The ventral angle (*Angulus ventralis*) was the most proeminent and complex of the angles (Figures 3 and 4). This is the location for the glenoid cavity (*Cavitas glenoidalis*) for the articulation of the humeral head. In this species, the glenoid cavity had a teardrop shape (elliptical) with the ventral portion being wider and the dorsal segment narrower (Table 2). The marginal edge of this cavity was found to be bordered peripherally with a supplementary cartilaginous rim named the articular labrum (*Labrum articulare*).

The area surrounding the glenoid cavity possessed several osseous processes, with important roles for the muscular origins (Fig. 4). Dorsal to the glenoid cavity, the supraglenoid tubercle (*Tuberculum supraglnoidale*) was visible. Well developed, this tubercle is the origin point for the long head of the biceps brachii muscle (*M. biceps brachii*). The coracoid process (*Processus coracoideus*) in *Chlorocebus sabaceus* was also prominent. This process can be described as an elongated bony prominence originating from the medial surface of the supraglenoid tubercle and curved ventrally on the medial aspect of the glenohumeral joint (Table 2). At the level of the proximal segment of the coracoid process, we could identify a smooth area for the attachment of coracoclavicular ligament (*ligamentum coracoclaviculare*) which serves as the point of origin for the coracobrachialis muscle.

Ventral to the glenoid cavity, the infraglenoid tubercle (*Tuberculum infraglenoidale*) was examined to find it significantly smaller than the supraglenoid tubercle and served as the origin point for the teres minor muscle (*m.teres major*). The coracoid process, acromial process, supraglenoid process and infraglenoid process, together with the muscles whose origins

Table 3

Comparison of measurements for association with sex (measures in mm)

Measurement	Male		Female		Difference of means male- female(%)
	Average value	Interval	Average value	Interval	
2	54.59	52.7-58.1	51.92	51.8-52.4	4.89
4	60.15	56-64.2	58.38	56.8-59.2	2.94
5	19.4	17.2-21.64	17.64	15.2-20.9	9.07
6	32.27	33.9-38.5	34.8	32.2-36.3	-7.84
7	75.71	71.3-81.22	69.41	65.05-72.19	8.32
8	65.55	62.8-70.52	59.35	55.3-63	9.46
9a	12.54	10.9-15	11.69	8.76-13.82	6.78
9b	4.638	4.19-5.37	4.40	4.73-4.12	5.13
10	12.83	10.8-14.29	12.20	11.32-13.68	4.91
11	4.35	3.97-5.16	3.985	3.32-4.3	8.39
12	24.12	18.37-32	21.28	18.56-24	11.77
13	5.12	3.96-6	4.58	4.45-4.71	10.55
14	11.018	8.64-14	10.035	7.15-12.61	8.92
15	7.01	5.06-13.8	9.69	6.75-12.79	-38.23
16	17.14	13.8-24.5	14.82	13.9-15.9	13.54
17	29.85	26.11-34.2	28.2	23.5-33.2	5.53

are here, have an important role in movement and stabilization of the glenohumeral joint.

The macroscopic aspects of the scapula of the *Chlorocebus sabaeus*, seem to fit somewhere intermediate between that of common domestic quadruped mammals and humans, very similar to the morphological description of the *S. leucopus* and other non-human primates. Due to the bipedal human locomotion and our anteroposterior compression of the rib cage, the anatomical position of the scapula and the terms utilized to describe it are inherently unique. Previous researchers have reported the posterior surface (*Facies posterior*) as homologue the lateral surface of the African green monkey and the anterior surface (*Facies anterior*) as similar to the costal surface of the scapula in quadrupedal mammals. Also, the names to describe the margins and angles are slightly different in human terminology (24, 25). The generally triangular shape of the scapula has been reported in domestic and wild mammal species (2, 7). The presence of the scapular spine is a common attribute of mammals; yet each species has visible morphological differences with unique proportions between the areas above and below the spine (the scapular fossae). This ratio also has a strong correlation with the mechanism of locomotion for each species (27). Compared with other species, the scapular spine in Chlorocebus sabaeus species was relatively straight and its thickness was largely constant throughout its length. This seems to be similar the that which has been reported in the macaque (*Macaca mulatta*) (26), common marmoset (*Callithrix jacchus*) (4, 24) and *S. leucopus* (14, 26, 24). In horses (*Equus caballus*), pigs (*Sus scrofa*), and Korean wild deer (*Hydropotes inermis argyropus*) a tuberosity of the scapular spine (*Tuber spinae scapulae*) has been well described previously [33,35,36]. Similarly, humans also possess this tuberosity; however, the associated terminology typically utilized is the deltoid tuberosity of the scapular spine (*Tuber deltoideus*) (24). This tuberosity was not visualized in studied species, like what is seen in carnivores (2, 12) . In contrast to the above descriptions, the scapular spine of ruminants presents with a more serpentine or wave appearance in its length from dorsal to ventral.

The distal end of the scapular spine in the studied species was similar that which has been reported in the white-maned tamarin (*Saguinus leucopus*), ring-tailed lemur (*Lemur catta*), humans (*Homo sapiens*), macaques (14, 26, 24) and dogs (*Canis familiaris*) (2) , and it seems that a well-developed acromial process (unossified in most of the monkeys species at the time of birth (22)) is specific for the terrestrial monkey (21, 1). In contrast, horses and pigs do not possess an acromion, but in ox, sheep, and goats, it presents a conical shape, and lacks a hamate process. In other species like cats (*Felis catus*), African lions (*Panthera leo*), tigers (*Panthera tigris*), leopards (*Panthera pardus*), rabbits(*Oryctolagus cuniculus*) the hamate and supra-hamate processes have been well described (24, 25).

In Rhesus monkeys, the scapular spine is the origin point for the spinodeltoideus muscle (*M. deltoideus, pars spinalis*) while the acromion is the origin site for the acro-miodeltoideus muscle (*M. deltoideus pars acromialis*). In the Black stripped capucin (*Cebus libidinosus*) this process is the origin for the infraspinatus muscle (M.infraspinati), long head of triceps brachii,

Table 4

Kolmogorov-Smirnov test values for measurements 14,15,16 and 17

Measurement no	Females	Males
14	not enough available measurements	D=0.16801., p-value= 0.89765
15	not enough available measurements	D= 0.23779, p-value=0.48993
16	not enough available measurements	D= 0.27609, p-value=0.42301
17	D= 0.22724, p-value= 0.72433	D=0.12974, p-value= 0.97192

and thoracic part of the trapezius muscle.

The morphometric ratio between the supraspinous fossa and infraspinous fossa was aproximately 1:2, which is similar to the values reported in the Rhesus macaque (*Macaca mulatta*), horses, pigs, and rabbits. In contrast, an approximate 1:1 ration has been reported in dogs and cats, and 1:3 in ruminants. In all species, these two fossae are the origin points for the supraspinatus (*M.supraspinati*) and the infraspinatus (*M. infraspinati*) muscles.

The medial surface of the scapula of the *Chlorocebus sabaeus* the facies serrata (*Facies serrata*) was absent in all specimens inspected; however, in dogs, this area has a generally rectangular shape on medial aspect of the cervical angle of the scapula. In horses and cows, the facies serrata takes on a more triangular shape located on the medial surface of the scapula near the the cranial and caudal scapular angles. This area represents the insertion point for the thoracic and cervical parts of the serratus ventralis muscle (*M. serratus ventralis*). Due to the lack of a proper facies serrata, in vervet monkeys, the origin point of serratus ventralis muscle is more similar to that reported in humans and S. leucopus, which is instead located on the medial side of the dorsal border of scapula .

The dorsal border of the scapula is convex in the vervet monkey and was covered by the scapular cartilage. This cartilage is very well developed in Artiodactyla and Perisodactila species and greatly reduced in carnivore species (14). There is a direct correlation between the size of scapular cartilage and the intensity of shock during foot ground impact for the forelimb [36, 38]. In lemurs this cartilage also serves as the origin for the rhomboideus muscle and is vital in its shock absorbing ability .

In *Chlorocebus sabaeus*, margo caudalis has had a double line characteristic, like reported in Goeldi's monkey (*Callimico goeldii*), *S. leucopus*, and *Macaca mulatta* species. According to the reported data, the medial bony line is the origin point for the subscapularis muscle (*M. subscapularis*), and the lateral line is the origin point for the long head of triceps, teres major and teres minor muscles. It was visible that the lateral line of the studied species is the more realistic caudal border. The cranial border of the scapula presented with similar features as the reported data in other quadrupedal mammals. The round cranial angle reported here seems to be an adaptation to the arboreal displacement correlated with large scapular mobility. A similar appearance has been reported in pigs, dogs, cats and primates. In horses and small and large ruminants, however, the cranial angle presents with a more acute angulation.

The coracoid process appears to be ossified in most primate species by the time of birth (22). In green monkeys, the coracoid process was very well developed, likely a function of the relatively robust development of the coracobrachialis muscle (*M. coracobrachialis*), and is likely due to its vital role in climbing and vertical movement of the scapula. In the Linnaeus's two-toed sloth (*Choloepus didactylus*), a more flared and wide acromial process is noted (20). In other domestic mammals, this process is more rudimentary, except in rabbits (*Oryctolagus cuniculus*) where a clearly well-developed coracoid process is visible.

The teardrop shape of the glenoid cavity described here in the *Chlorocebus sabaeus*, is similar to the piriform appearance of *Saguinus oedipus* and *S. eucopus*. A more oval shape to the glenoid cavity is reported in the Ateles genus (24).

As we can see in the table, most values indicate a positive association between lengths of bone prominences likelihood of the males' sex. In general (although due to the reduced sample-size, we should treat these values with some reserves), a 3-10% difference was observed in all, except for 3 measurements compared to those of female measurements (Table 3).

Only the width from the coracoid process to the acromion (measurement 17) allowed for use of ANOVA / Tukey test (although from a very limited number of values, thus the reserve in interpretation), proving the compared value sets to be insignificant in respect to length (f- ratio = 1.17932 with p-value = 0.29385).

Despite the limited number of measurements available, a relevant set of indices was calculated, taking into account the relevance of the same indices in humans. The length-to-width ratios of the scapulas at their maximal were calculated (width-length index) and can be seen in measurements no 7 and 9a as expressed as percent proportions. The glenoid cavity index was calculated in the same fashion and is seen as the percent ratio of comparing measurements 16 and

Table 5

Calculation of different scapular indices (averages) and the male-female distribution of values

Index	Average value (all specimens)	Average values and intervals for males	Average values and intervals for females
Scapular width-length index	5.96	6.03	5.93
Glenoid cavity index	1.52	1.55	1.47
Scapular length and scapular width index	0.94	0.91	0.98
Supraspinous-infraspinous fossa ratio (1/X)	1:2.07	1:2.35	1:1.99
Absolute surface area of the acromion	55.78	58.06	51.43
Surface area of the acrominal area (measured)	54.68 mm^2	54.33 mm^2	54.42 mm^2
Surface area for teres major (measured)	129.3 mm^2	142.3 mm^2	11.4 mm^2
Surface area of the supraspinous fossa (measured)	533.2 mm^2	571.9 mm^2	458.8 mm2
Surface area of the subspinous fossa (measured)	1113.1 mm^2	1209.0 mm^2	993.1 mm^2
Ratio of the measured surfaces of the supraspinous and subspinous fossae	1:2.138	1:2.149	1:2.12

14. Finally, a ratio of measurements of scapular length to morphological width ratio was calculated (measurements 4 and 8).

Another interesting calculation was undertaken to assess the absolute area of the acromion process expressed as a product of the length and width (9a and 9b). This measurement has been established previously (used as a reference in other research papers (6, 8). The area for the insertion of the teres major muscle, the infraspinous, and supraspinous fossae was also measured in a similar fashion (expressed as area computed with the ImageJ® polygonal tool).Due to the fact that only 10 total scapulas were measured, the expression of variability was not attained for these values, and their average is provided instead (Table 5).

The area of the acromion (expressed in mm^2) (18) as calculated by measurement of surface area, is a key element of primate scapular research, because of its relationship in humans and other hominids to the biomechanics of the deltoid muscle in its ability to cause abduction at the shoulder. This area of research is largely related to the pathology of human rotator cuff tears at its acromial insertion. The absolute physical area of the acromion does not differ significantly from the area of an overlapped polygonal shape using the ImageJ software. This proves some correlation to the estimate of the area for the insertion of the deltoid muscle. Even though the average values are similar, the above-mentioned results seem to provide minor differentiation between sexes (over 10% higher values for males, Table 4). The importance of the insertion area of the teres major muscle resides in its functionality in its role in rotation and adduction of the humerus, or its extension backwards and downwards, thus providing strength in climbing movements in several primate species (24). As illustrated in Table 3, there is a higher than 25% difference for males than females in absolute values of the insertion area for this muscle, likely associated with differences in muscle mass between sexes. The importance of the subspinous area is correlated to the subspinous muscle as a protector and stabiliser of the shoulder joint, in its ability to cause rotation and adduction at the shoulder, respectively, the arm forward and downward functionality. The *m. supraspinosus*, in its role as an abductor of the arm, plays a similar protective role as the shoulder joint by pulling the humeral head medially. In the biomechanics of the primate shoulder, all these muscles play a significant role in the direction and magnitude of forces that act on the humeral head, glenoid joint, and thoraco-scapular junction. The area values for their respective insertion sites also prove a significant difference between sexes (between 20% - 25% higher values for males vs. females) (Tables 4 and 5).

Another interesting finding was related to the dimensions of the subspinous and supraspinous fossae's, pointing to some proportional differences among sexes when the absolute areas of the muscle's

insertions are taken into consideration (Table 5).

CONCLUSIONS

Our investigation of the scapula in *Chlorocebus sabaeus* revealed several physical features directly related to terrestrial locomotion, and it has many similarities with other quadrupedal species. Due to the anatomical-topographical structures of the scapula described here, a correct anatomical description of the terms of Nomina Anatommica Veterinaria is recommended. The robust development of some structures, such as the acromion process, supraglenoid process, and the area of origin for the teres major muscle, reveals the important role of specific muscles in locomotion. Although the studied species is a terrestrial one, the morphological structure of the cranial angle highlights an important adaptation to arboreal locomotion. This data may serve to compare measurements to those of primates and other mammalian species. The present investigation provides assessments of raw metrical data on several measurable elements of the scapula in the green monkey. Comparisons of this metrical data illustrate some intricate differences among sexes, while other indices are not significant. Indirect calculations may also serve as interesting starting points for comparing different locomotion patterns for other mammal species.

Acknowledgments

The publication was partly supported by funds from the National Research Development Projects to Finance Excellence (PFE)-14 (ID 546) granted by the Romanian Ministry of Research, Innovation and Digitalization. The animal study protocol was approved by the Animal Care and Use Committee (IACUC) (TSU 10.27.2023 CM RUSVM) Ross University School of Veterinary Medicine (RUSVM), Saint Kitts and Nevis, Basseterre.

Conflict of interest statement

The authors declare no conflict of interest. The funders had no role in the design of the study; in the collection, analyses, or interpretation of data; in the writing of the manuscript; or in the decision to publish the results.

REFERENCES

1. *Alghazaly H.M., El-Ghazali H.M., El-Behery E.I.,* (2018), Comparative macro-anatomical observations of the appendicular skeleton of New Zealand rabbit (*Oryctolagus cuniculus*) and domestic cat (*Felis domestica*) thoracic limb. Inter J Vet Sci, 7(3):127-133
2. *Barone R.,* (1966), Anatomie comparée des Mammifères domestiques, Tome 1, Ostéologie. 3e ed. [Comparative Anatomy of Domestic Mammals, Volume 1, Osteology. 3rd ed.], Vigot, Paris.
3. *Bouskila J., Javadi P., Palmour R.M., Bouchard J.F., Ptito M.,* (2014), Standardized full-field electroretinography in the green monkey (*Chlorocebus sabaeus*). PLoS One, 9:e111569
4. *Casteleyn C., Bakker J., Breugelmans S., Kondova I., Saunders J., Langermans J.A.M., Cornillie P., Van den Broeck W., Van Loo D., Van Hoorebeke L., Bosseler L., Chiers K., Decostere A.,* (2012), Anatomical description and morphometry of the skeleton of the common marmoset (*Callithrix jacchus*). Lab Anim, 46(2);152-163
5. *Casteleyn C., Gram C., Bakker J.,* (2023), Topographical Anatomy of the Rhesus Monkey (Macaca mulatta)—Part I: Thoracic Limb. Veterinary Sciences, 10:164
6. *Ciochon R.L., Corruccini R.S.,* (1977), The coracoacromial ligament and projection index in man and other anthropoid primates. J Anat, 124:627-632
7. *Dyce K.M., Sack O.W., Wensig C.J.G.,* (2010), Textbook of Veterinary Anatomy, 4th edition, (Ed.) Saunders Elsevier, St Louis, Missoury, USA
8. *Fujisawa Y., Mihata T., Murase T., Sugamoto K., Neo M.,* (2014), Three-dimensional analysis of acromial morphologic characteristics in patients with and without rotator cuff tears using a reconstructed computed tomography model. American Journal of Sports Medicine, 42:2621–2626
9. *Georgescu B., Rosu P.M., Belu C.R., Visoiu C., Mustatea A.I.,* (2023), The chimpanzee skull (*Pan Troglodytes*, Blumenbach, 1775): Case Study. Revista Romana de Medicina Veterinara, 33(2):29-34
10. *Green D.J., Chirchir H., Mbua E., Harris J.W.K., Braun D.R., Griffin N.L., Richmond B.G.*, (2018), Scapular anatomy of Paranthropus boisei from Ileret, Kenya. J Hum Evol, 125:181-192
11. *Jasinska A.J., Service S., Levinson M., Slaten E., Lee O., Sobel E., Fairbanks L.A., Bailey J.N., Jorgensen M.J., Breidenthal S.E., Dewar K., Hudson T.J., Palmour R., Freimer N.B., Ophoff R.A.,* (2007), A genetic linkage map of the vervet monkey (*Chlorocebus aethiops sabaeus*). Mammalian Genome, 18:347-360
12. *Konig H.,* (2004), Veterinary Anatomy of Domestic Mammals, 4th Edition, (Ed.)Schattauer, Stuttgart, Germany
13. *Van Der Kuyl A.C., Dekker J.T., Goudsmit J.,* (1996), St. Kitts green monkeys originate from West Africa: Genetic evidence from feces. Am J Primatol, 40:361-364.
14. *Makungu M., Groenewald H.B., du Plessis W.M., Barrows M., Koeppel K.N.,* (2015), Thoracic Limb Morphology of the Ring-tailed Lemur (*Lemur ca-*

tta) Evidenced by Gross Osteology and Radiography. Anat Histol Embryol, 44:288-298
15. *Martonos C.O., Gudea A.I., Ratiu I.A., Stan F.G., Bolfă P., Little W.B., Dezdrobitu C.C.,* (2023), Anatomical, Histological, and Morphometrical Investigations of the Auditory Ossicles in *Chlorocebus aethiops sabaeus* from Saint Kitts Island. Biology (Basel), 12(4):631
16. *Michilsens F., Vereecke E.E., D'Août K., Aerts P.,* (2009), Functional anatomy of the gibbon forelimb: adaptations to a brachiating lifestyle. J Anat, 215:335-354
17. *Mikula S., Stone J.M., Jones E.G.,* (2008), Brain Maps.org - Interactive High-Resolution Digital Brain Atlases and Virtual Microscopy. Brains Minds Media, 3, bmm1426.
18. *Moor B.K., Wieser K., Slankamenac K., Gerber C., Bouaicha S.,* (2014), Relationship of individual scapular anatomy and degenerative rotator cuff tears. J Shoulder Elbow Surg, 23:536-541
19. *Mrożek K., Marchewka J., Leszczyński B., Wróbel A., Głąb H.* (2020) Variability in the number of mental foramina in the African green monkey (Grivet) (*Chlorocebus aethiops*). Zoomorphology, 139:393-405
20. *Nyakatura J.A., Fischer M.S.,* (2010), Three-dimensional kinematic analysis of the pectoral girdle during upside-down locomotion of two-toed sloths (*Choloepus didactylus*, Linné 1758). Front Zool, 7:21-21
21. *Preuschoft H., Hohn B., Scherf H., Schmidt M., Krause C., Witzel U.,* (2010), Functional analysis of the primate shoulder. Int J Primatol, 31:301-320
22. *Smith T.D., DeLeon V.B., Vinyard C.J., Young J.W.,* (2020), The Pectoral Girdle and Forelimb Skeleton. In: Skeletal Anatomy of the Newborn Primate, (Ed.) Cambridge University Press, Cambridge, UK, 163-190
23. *Spataru M.C., Gradinaru A.C., Spataru C.,* (2023), The suitability of using the ferret as a model organism in biomedical research. Revista Romana de Medicina Veterinara, 33:50-54
24. *Vélez-García J.F., Monroy-Cendales M.J., Castañeda-Herrera F.E.,* (2019), Morphometric, anatomic and radiographic study of the scapula in the white-footed tamarin (*Saguinus leucopus*): report of scapular cartilage and one variation in cranial (superior) transverse scapular ligament. J Anat, 234:120-131
25. *Vélez-García J.F., Torres-Suárez S.V., Echeverry-Bonilla D.F.,* (2020), Anatomical and radiographic study of the scapula in juveniles and adults of *Tamandua mexicana* (Xenarthra: Myrmecophagidae). Journal of Veterinary Medicine Series C: Anatomia Histologia Embryologia, 49:203-215
26. *Verma A., Pathak A., Prakash A., Farooqui M., Singh S.,* (2017), Functional Anatomy of Scapula of Monkey (*Macaca mulatta*). International Journal of Livestock Research, 7(9):69-74
27. *Voisin J.L., Ropars M., Thomazeau H.,* (2014), The human acromion viewed from an evolutionary perspective.Orthopaedics and Traumatology: Surgery and Research, 100:S355–S360.
28. *Waibl H., Gasse H., Constantinescu G., Hashimoto Y., Simoens P.,* (2017), Nomina Anatomica Veterinaria 6th edition, International Committee, Veterinary Gross Anatomical Nomenclature (eds) ICV GAN, Hanover (Germany), Ghent (Belgium), Columbia, MO (U.S.A.), Rio de Janeiro (Brazil).